

# Enhancement of thermal buckling strength of laminated sandwich composite panel structure embedded with shape memory alloy fibre

Pankaj V. Katariya<sup>1a</sup>, Subrata K. Panda<sup>\*1</sup>, Chetan K. Hirwani<sup>1b</sup>,  
Kulmani Mehar<sup>1c</sup> and Omprakash Thakare<sup>2d</sup>

<sup>1</sup>Department of Mechanical Engineering, NIT Rourkela, Rourkela-769008, Odisha, Sundergarh, India

<sup>2</sup>Department of Mechanical Engineering, G.D. Rungta College of Engineering, Bhilai, Chhatisgarh, India

(Received June 15, 2017, Revised August 15, 2017, Accepted August 17, 2017)

**Abstract.** The present article reported the thermal buckling strength of the sandwich shell panel structure and subsequent improvement of the same by embedding shape memory alloy (SMA) fibre via a general higher-order mathematical model in conjunction with finite element method. The geometrical distortion of the panel structure due to the temperature is included using Green-Lagrange strain-displacement relations. In addition, the material nonlinearity of SMA fibre due to the elevated thermal environment also incorporated in the current analysis through the marching technique. The final form of the equilibrium equation is obtained by minimising the total potential energy functional and solved computationally with the help of an original MATLAB code. The convergence and the accuracy of the developed model are demonstrated by solving similar kind of published numerical examples including the necessary input parameter. After the necessary establishment of the newly developed numerical solution, the model is extended further to examine the effect of the different structural parameters (side-to-thickness ratios, curvature ratios, core-to-face thickness ratios, volume fractions of SMA fibre and end conditions) on the buckling strength of the SMA embedded sandwich composite shell panel including the different geometrical configurations.

**Keywords:** buckling analysis; sandwich panel; SMA; HSDT; FEM

## 1. Introduction

Since last several decades, the demand for the lighter and the stronger materials with tailored-made properties have been increased. In this regard, the sandwich structures (two face sheet separated with core either same or different material) are highly preferred due to their load bearing capacity and unlike the deformation characteristics of the different components. In today's modern engineering, the sandwich components have received enormous attention owing to their specific features. These structural components employed in different industries like aviation to automotive and generally under the influence of the combined types of loadings (aerostatic, dynamic and aerodynamic heating) during their service. This may result in large deformation of the structural geometries and attend the acute condition when exposed to the complex loading, especially elevated temperature environment. The structural components are prone to buckle under the excess thermal loading and lose their stability because of the large geometrical distortion. Further, the rise in temperature adversely affects the load-carrying capacity of the structure

or structural members. Hence, the buckling analysis of the sandwich structure becomes important to examine from the design point of view. Further, to take care the large deformation of the structural component two types of strain-displacement relations are implemented for the analysis purpose and to predict the responses accurately. Subsequent development in the advanced functional materials and ease of fabrication improvises the structural capabilities. These materials are intelligent enough to sense the adverse conditions and actuate according to the system requirement without increasing the weight penalty. In general, the materials have functional characteristics called the smart or the intelligent materials. These smart materials have good capability to change the shape, stiffness, frequency as well as other mechanical responses with respect to the change in the external stimuli i.e., the temperature, the electric and/or the magnetic fields. There are various smart materials are available at present days like shape memory alloys (SMAs), magnetostrictive materials, piezoelectric materials, magnetorheological fluids and electrorheological fluids. For the present research, SMAs have been ingeniously embedded with the sandwich structural panel to increase the buckling load strength.

In the past, many researchers have adopted different solution techniques including the theories to compute the buckling behaviour of the laminated as well as the sandwich structural panel and few important contributions are discussed in the upcoming lines to establish the necessity of the current analysis. The stability responses of laminated and sandwich composite cylindrical shell panels are investigated numerically using Galerkin approach and the

\*Corresponding author, Ph.D.

E-mail: call2subrat@gmail.com

<sup>a</sup> E-mail: pk.pankajkatariya@gmail.com

<sup>b</sup> E-mail: chetanhirwani111@gmail.com

<sup>c</sup> E-mail: kulmanimehar@gmail.com

<sup>d</sup> E-mail: omprakashthakare82@gmail.com

finite element method (FEM) by Sciuva and Carrera (1990) with the help of Mindlin theory. Further, Love's first approximation theory is adopted by Birman (1997a, b) to study the stability responses of the composite and functionally graded (FG) sandwich structures embedded with SMA fibres under thermo-mechanical loading. In addition, the thermal buckling behaviour of the laminated composite and sandwich plate are investigated by Babu and Kant (2000) and Kant and Babu (2000) including the skew angle of fibre to explore the generality of proposed analysis based on different shear deformation kinematics (first-order shear deformation theory; FSDT and higher-order shear deformation theory; HSDT). A finite element (FE) simulation model is developed by Lee and Lee (2000) with the help of a commercial numerical tool (ABAQUS) to investigate the bifurcation responses and the post-buckling strength of the laminated composite shell structures reinforced with SMA wires. Subsequently, the FSDT kinematics has been adopted to study the nonlinear frequencies and the post-buckling load parameter of the laminated composite plate structure embedded with SMA fibres (Park *et al.* 2004, Zhang and Zhao 2007a, b) with the help of finite element method (FEM) in association with von-Karman type of geometrical nonlinearity. In recent past, the FEM is employed to examine the effect of SMA fibres on the buckling strength of the rectangular composite laminate based on three-dimensional (3D) layer-wise theory (LWT) by Kuo *et al.* (2009) and Kumar and Singh (2009). Further, the optimal design parameters of the laminated cylindrical shell structure are predicted by Topal and his co-authors (2009a, b, 2012) using the modified feasible direction (MFD) technique and the FSDT kinematics under the uniformly distributed temperature load. The vibration and buckling characteristics of the FG sandwich plate structure are reported by Bourada *et al.* (2011) and Meiche *et al.* (2011) using a new hyperbolic displacement model including the geometrical distortion via von-Karman type of strain kinematics in the framework of the refined plate theory (RPT). Further, the mechanical responses of the graded, laminated composite and sandwich structures are evaluated by Kaci *et al.* (2013) and Kettaf *et al.* (2013) using a new hyperbolic displacement model in the framework of the RPT including von-Karman strain kinematics. Similarly, the responses are investigated by Thai *et al.* (2013) using the non-uniform rational B-spline (NURBS) technique in association with an isogeometric approach in the framework of the LWT. Fazzolari and Carrera (2013) developed the theoretical model of the laminated composite and the sandwich structures using an extended framework of Carrera's Unified Formulation (CUF) and computed the buckling strength numerically with the help of Ritz and Galerkin methods. In recent past, the nonlinear free vibration frequency responses of the thermally post-buckled laminated composite spherical shell panel embedded with SMA fibre are investigated numerically by Panda and Singh (2013) using the FEM technique. The shell panel model is developed using the HSDT mid-plane theory and the nonlinear strain kinematics due to the temperature environment is introduced in the model via Green-Lagrange relations. Further, the static and

dynamic responses of the arbitrarily shaped structures (rod, beam, membrane and plate) are analysed by Tornabene *et al.* (2014) using the strong formulation finite element method (SFEM) in conjunction with the Differential Quadrature Method (DQM). The recovery of stress-strain and the bifurcation characteristics of the laminated and doubly-curved FG sandwich structures are examined using GDQ technique by Chalak *et al.* (2015) and Tornabene *et al.* (2015) with the help of CUF model including the generalized higher-order zig-zag theory (HOZT).

Now, few studies related to the application of the functional materials including the subsequent enhancement of the laminated and the sandwich structural strength are discussed to elaborate the necessity of the current research. The necessary improvement in the thermal buckling strength of the layered cylindrical shell structure is examined numerically by Asadi *et al.* (2015) by embedding SMA fibre with the help of Birman's constitutive model and von-Karman nonlinear strain-displacement relations. Further, the dynamic and the stability behaviour of the delaminated composite and sandwich laminated plate are analysed (Juhász and Szekrenyes 2015a, b, Dehkordia and Khalili 2015) using the established FEM technique via CUF in conjunction with Kirchhoff's plate theory. The piezoelectric layer is employed as the smart layer by Singh and Panda (2015) to reduce the nonlinear frequency responses of the laminated composite shell panel and the desired responses are computed numerically using the HSDT mid-plane theory in association with Green-Lagrange strain kinematics. Recently, the nonlinear frequency values of the laminated composite shell panel embedded with SMA fibre reported by Parhi and Singh (2016) using the geometrical nonlinearity via von-Karman sense and the HSDT kinematics. In addition, the buckling and the flutter behaviour of the laminated composite and the FG sandwich structures embedded with and without SMA fibres are investigated (Shao *et al.* 2016, Boudarba *et al.* 2016, Hassanli and Samali 2016, Katariya and Panda 2016, Chikh *et al.* 2017) via the established mid-plane kinematic theories (classical plate theory, the FSDT and the HSDT) including the common types of strain-displacement relation (von-Karman and Green-Lagrange) for the inclusion of geometrical distortion. Fantuzzi *et al.* (2017) reported the buckling strength of the laminated structure using Fourier-based strong form approaches (harmonic DQM, Fourier DQM and improved Fourier expansion-based DQM) in the framework of Reissner-Mindlin plate theory to ensure the reliability of the numerical analysis.

The cursory look over the comprehensive literature indicates that sincere efforts have already been made in the past to indicate the necessary techniques including the accuracy of the buckling analysis of the sandwich structural components with or without SMA fibre under elevated environment. However, it is interesting to note that no study reported yet on the thermal buckling strength prediction of the SMA embedded sandwich shell panel using the HSDT mid-plane kinematics in conjunction with Green-Lagrange strain-displacement relations for the inclusion of the large structural distortion under the elevated thermal environment. Based on the available research gap, the

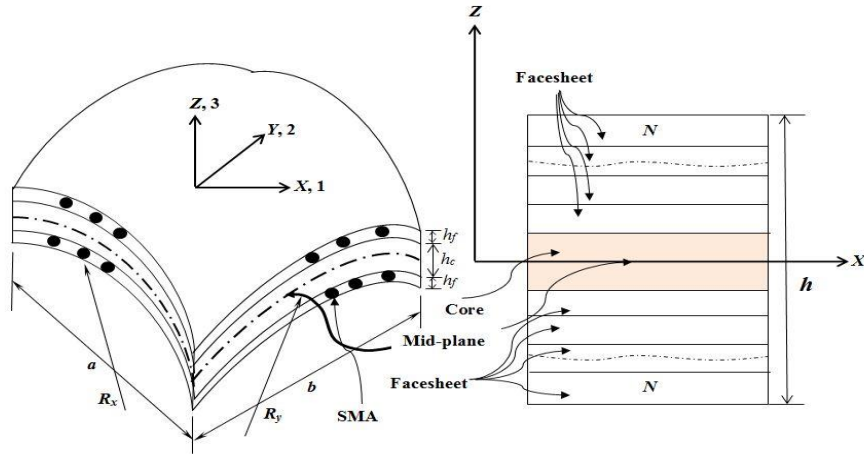


Fig. 1 Configuration of the laminated sandwich composite shell panel embedded with SMA fibres

present article aims to develop a generalised higher-order numerical model for the analysis of thermal buckling responses of SMA embedded sandwich shell panel structure and subsequent improvement due to the functional material under the elevated thermal field. In addition, the current model includes all of the higher-order nonlinear terms due to the large distortion in geometry under the elevated thermal load. Subsequently, the desired buckling responses are computed with the help of an original MATLAB code using the current higher-order FEM model. The solutions are obtained via minimizing the total potential energy functionals. Finally, the effect of the different geometrical design parameters (side-to-thickness ratio, curvature ratio, core-to-face thickness ratio, the volume fraction of SMA fibre and support condition) on the buckling strength of the SMA embedded layered sandwich structure computed numerically using the current higher-order model and their importance in the current domain discussed in details.

**2. Mathematical modelling**

The layered sandwich composite shell panel embedded with SMA fibre is presented in Fig. 1, for the clear understanding and implementation purpose. Now, the geometrical dimension of the sandwich shell panel is considered as length ‘a’, width ‘b’ and the total thickness ‘h’ whereas the total thickness is the sum of two components i.e., the thickness of core ‘h<sub>c</sub>’ and the thickness of the face sheet ‘h<sub>f</sub>’. In addition, the necessary curvature related parameters say, ‘R<sub>x</sub>’ and ‘R<sub>y</sub>’ are the principal radii of curvature in the respective directions introduced in the current modelling to achieve the desired geometries of the sandwich shell panel by taking suitable value. The shell geometry classifications are broadly based on their curvature parameter, i.e., spherical (R<sub>x</sub> = R and R<sub>y</sub> = R), hyperbolic (R<sub>x</sub> = R and R<sub>y</sub> = -R), elliptical (R<sub>x</sub> = R and R<sub>y</sub> = 2R), cylindrical (R<sub>x</sub> = R and R<sub>y</sub> = ∞) and flat (R<sub>x</sub> = ∞ and R<sub>y</sub> = ∞) instead of their load bearing capacity.

**2.1 Displacement field**

Now, the displacement field kinematics for any structure i.e., the laminated sandwich composite shell panel embedded with SMA fibre for current analysis are expressed based on the higher-order mid-plane kinematics with ten degrees-of-freedom per node as in Katariya and Panda (2016)

$$\left. \begin{aligned} u &= u_0 + z\theta_x + z^2\phi_x + z^3\psi_x \\ v &= v_0 + z\theta_y + z^2\phi_y + z^3\psi_y \\ w &= w_0 + z\theta_z \end{aligned} \right\} \quad (1)$$

where, (u, v, w) and (u<sub>0</sub>, v<sub>0</sub>, w<sub>0</sub>) are the displacement and the mid-plane displacement of any point within the shell panel along x, y and z directions, respectively. The rotation of normal to the mid-plane and extension are considered as (θ<sub>x</sub>, θ<sub>y</sub>) and θ<sub>z</sub>, respectively. The functions φ<sub>x</sub>, φ<sub>y</sub>, ψ<sub>x</sub> and ψ<sub>y</sub> are higher order terms of Taylor series expansion in the mid-plane of the shell panel.

**2.2 Strain-displacement field**

The generalised strain-displacement relations utilised for the present SMA embedded sandwich shell structure as in Katariya and Panda (2016)

$$\{\varepsilon\} = \begin{Bmatrix} \varepsilon_{xx} \\ \varepsilon_{yy} \\ \varepsilon_{zz} \\ \gamma_{yz} \\ \gamma_{xc} \\ \gamma_{xy} \end{Bmatrix} = \begin{Bmatrix} \frac{\partial u}{\partial x} + \frac{w}{R_x} \\ \frac{\partial v}{\partial y} + \frac{w}{R_y} \\ \frac{\partial w}{\partial z} \\ \frac{\partial v}{\partial z} + \frac{\partial w}{\partial y} - \frac{v}{R_y} \\ \frac{\partial u}{\partial z} + \frac{\partial w}{\partial x} - \frac{u}{R_x} \\ \frac{\partial u}{\partial y} + \frac{\partial v}{\partial x} + 2\frac{w}{R_{xy}} \end{Bmatrix} \quad (2)$$

### 2.3 Mechanics of SMA embedded laminated sandwich composite matrix

In general, SMA is associated with four characteristic stable state temperatures during the solid state phase transformation as shown in Fig. 2. The temperatures are namely, Martensite start ( $M_s$ : temperature at which the SMA begins transforming from the austenite to martensite), Martensite finish ( $M_f$ : temperature at which the SMA becomes fully martensitic), austenite start ( $A_s$ : represents the temperature at which the ‘‘reverse transformation’’ begins) and austenite finish ( $A_f$ ) represents the temperature at which the SMA is fully in austenitic phase. In addition, SMA exhibit twinned and detwinned molecular configurations, which, in turn, allows to accommodate the mechanical deformation within the structure and returned to the original state when exposed to the elevated thermal loading under the free-free condition. However, SMA produces the recovery stress under the influence of the temperature loading at the constraint condition when bonded with epoxy (Panda 2009) and such phenomena called shape memory effect (SME).

Now, the elastic properties along the principal material directions of the current panel say, 1, 2 and 3 are presented in Fig. 1. The necessary elastic properties of SMA fibres are defined by assuming the uniform distribution of SMA within each layer and bonded closely with the composite lamina. The normal and transverse moduli including other necessary parameters of the SMA embedded sandwich shell panel structure are expressed as same as Panda and Singh (2013)

$$\left. \begin{aligned} E_1 &= E_{1m} V_m + E_{SMA} V_{SMA} \\ E_2 &= E_{2m} E_{SMA} / (E_{2m} V_{SMA} + E_{SMA} V_m) \\ G_{12} &= G_{12m} G_{SMA} / (G_{12m} G_{SMA} + G_{SMA} V_m) \\ G_{23} &= G_{23m} V_m + G_{SMA} V_{SMA} \\ \nu_{12} &= \nu_{12m} V_m + \nu_{SMA} V_{SMA} \\ \alpha_1 &= (E_{1m} \alpha_{1m} V_m + E_{SMA} \alpha_{SMA} V_{SMA}) / E_1 \\ \alpha_2 &= \alpha_{2m} V_m + \alpha_{SMA} V_{SMA} \end{aligned} \right\} \quad (3)$$

where, subscript ‘ $m$ ’ indicate the composite matrix.  $E$ ,  $G$ ,  $\nu$  and  $\alpha$  are Young’s modulus, the shear modulus, Poisson’s ratio and the thermal expansion co-efficient, respectively. Further,  $V_m$  and  $V_{SMA}$  are the volume fractions of the matrix and SMA fibre, respectively.

### 2.4 Constitutive relations

The stress-strain relations for the  $k$ th orthotropic lamina of SMA embedded sandwich composite matrix in material co-ordinate axes subjected to uniform temperature field are expressed as Panda and Singh (2013)

$$\{\sigma\}^k = [\bar{Q}]^k \{\varepsilon\}^k + \{\sigma_{\Delta r}\}^k V_{SMA}^k - \left( [\bar{Q}]_m \{\alpha\}_m V_m \right)^k \Delta T \quad (4)$$

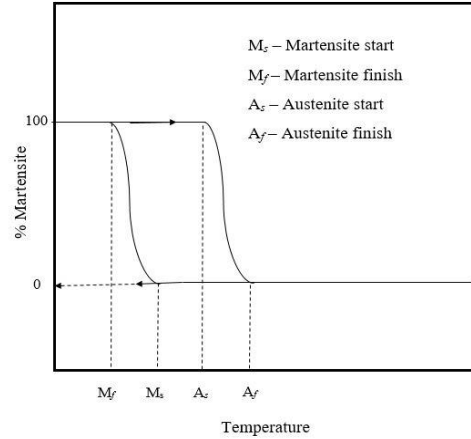


Fig. 2 Reverse Transformation of SMA

where,  $\{\sigma\}^k = \{\sigma_1 \ \sigma_2 \ \sigma_3 \ \sigma_4 \ \sigma_5 \ \sigma_6\}^T$  is the total stress vector measured at the stress-free state at  $T_{ref}$ ,  $\{\sigma_{\Delta r}\}$  is the recovery stress generated in SMA fibre due to the temperature increment  $(\Delta T)$  and  $\{\varepsilon\}^k = \{\varepsilon_1 \ \varepsilon_2 \ \varepsilon_3 \ \varepsilon_4 \ \varepsilon_5 \ \varepsilon_6\}^T$  is the strain vector, for the  $k^{th}$  layer. In addition,  $[\bar{Q}]^k$ ,  $[\bar{Q}]_m^k$  and  $\{\alpha\}_m^k = \{\alpha_{1m} \ \alpha_{2m} \ 2\alpha_{12m}\}^T$  are the transferred reduced stiffness matrix of SMA embedded lamina, transferred reduced stiffness matrix of the sandwich composite matrix and the transformed thermal expansion coefficient vector for the  $k^{th}$  layer, respectively.  $\Delta T$  is the uniform temperature difference.

Thermal in-plane generated forces can be obtained by integrating the Eq. (4) over the thickness of the shell panel and can be expressed in matrix form as follows

$$\begin{Bmatrix} \{N_{\Delta r}\} \\ \{M_{\Delta r}\} \\ \{P_{\Delta r}\} \end{Bmatrix} - \begin{Bmatrix} \{N_{\Delta r}\} \\ \{M_{\Delta r}\} \\ \{P_{\Delta r}\} \end{Bmatrix} = \quad (5)$$

$$\sum_{k=1}^N \int_{z_{k-1}}^{z_k} \{\sigma_{\Delta r}\}^k V_{SMA}^k - [\bar{Q}]_m^k \begin{Bmatrix} \alpha_{1m} \\ \alpha_{2m} \\ 2\alpha_{12m} \end{Bmatrix} (1, z, z^3) V_m \Delta T dz$$

where,  $\{N_{\Delta r}\}$ ,  $\{M_{\Delta r}\}$  and  $\{P_{\Delta r}\}$ , are the resultant vectors of compressive in-plane forces, moments and the higher order terms due to the temperature change  $(\Delta T)$  in composite matrix. In addition to that,  $\{N_{\Delta r}\}$ ,  $\{M_{\Delta r}\}$  and  $\{P_{\Delta r}\}$  are generated in SMA fibres due to the recovery stress  $\{\sigma_{\Delta r}\}$ .

The strain energy ( $U$ ) of the laminated sandwich composite shell panel can be expressed as

$$U = \frac{1}{2} \int_V \{\varepsilon\}^T \{\sigma\} dV \quad (6)$$

The total work done due to the resultant in-plane as well

as recovery forces can be expressed as

$$W = \frac{1}{2} \int_A \{\varepsilon_G\}^T [D_G] \{\varepsilon_G\} dA \quad (7)$$

where,  $\{\varepsilon_G\}$  represents the geometric strain and  $[D_G]$  represents the material property matrix.

### 2.5 Finite element formulation

FEM is a well established numerical tool for the analysis of the layered structure due to their geometrical and the material complexities. In this analysis, a displacement based FEM is adopted and the necessary discretisation of the domain obtained via a nine-noded quadrilateral isoparametric element with ten degrees of freedom (DOF) per node. The displacement field model  $\{\delta_0\}$  is further expressed in the following lines

$$\{\delta_0\} = \sum_{i=1}^9 N_i \{\delta_{0i}\} \quad (8)$$

where,  $\{\delta_{0i}\} = [u_{0i}, v_{0i}, w_{0i}, \theta_{xi}, \theta_{yi}, \theta_{zi}, \phi_{xi}, \phi_{yi}, \psi_{xi}, \psi_{yi}]^T$  is the nodal displacement field vector and  $N_i$  is the interpolating functions associated with the 'i<sup>th</sup>' node.

Now, the mid-plane strain vector in terms of the nodal displacement vector can be written as

$$\{\bar{\varepsilon}\} = [B] \{\delta_0\} \quad (9)$$

where,  $[B]$  is product form of differential operators and shape functions in the strain terms.

The elemental strain energy and the work done due to temperature loading are obtained by substituting the values of stress and strains in Eqs. (6) and (7) including Eqs. (8) and (9) and represented as

$$U^e = \frac{1}{2} \int_A \left( \{\delta_0\}_i^T [K]^e \{\delta_0\}_i \right) dA + \{F_{\Delta T}\}_i - \{F_{\Delta T}\}_i \quad (10)$$

$$W^e = \frac{1}{2} \int_A \left( \{\delta_0\}_i^T [K_G]^e \{\delta_0\}_i \right) dA \quad (11)$$

where,  $[K]^e = \int_{-1}^1 \int_{-1}^1 [B]_i^T [D][B]_i |J| d\xi d\eta$ ,  $\{F_{\Delta T}\}_i^e = \int_A [B]_i^T \{N_{\Delta T}\} dA$ ,  $\{F_{\Delta T}\}_i^e = \int_A [B]_i^T \{N_{\Delta T}\} dA$ ,  $[K_G]^e = \int_{-1}^1 \int_{-1}^1 [B_G]_i^T [D_G][B_G]_i |J| d\xi d\eta$ .  $[K_G]^e$  represents the elemental geometric stiffness matrix.  $[B]$  and  $[B_G]$  are the product form of the differential operator and nodal interpolation function in the linear strain terms and geometric strain terms, respectively.

### 2.6 Governing equations

Finally, the governing equation of the thermally buckled SMA embedded sandwich shell panel is obtained by minimizing the total potential energy (TPE) functional and

expressed as

$$\delta \Pi = 0 \quad (12)$$

where,  $\Pi = U^e + W^e$

Now, the final form of the equilibrium equation of the buckled sandwich composite shell panel embedded with SMA fibre can be obtained by substituting Eqs. (10) and (11) in Eq. (12) and rewritten as

$$([K_S] - T_{cr}[K_G])\{\delta_0\} = 0 \quad (13)$$

where,  $[K_S] = ([K] + [K_{\Delta r}])$  and  $[K_G]$  are the global stiffness matrix and global geometrical stiffness whereas  $[K_{\Delta r}]$  is the stiffness due to recovery stress behaviour of SMA. In addition,  $T_{cr}$  represents the critical buckling temperature load.

## 3. Results and discussion

In the present article, the buckling responses of SMA embedded sandwich shell panel are investigated numerically using the currently developed higher-order FE model. The responses are computed numerically by discretising the domain via a nine-noded isoparametric Lagrangian element with ten degrees of freedom at each node. The responses are obtained using an original home-made computer code developed in MATLAB environment with the help of the proposed higher-order numerical model in conjunction with FEM and marching technique (material nonlinearity in SMA). It is important to mention that elastic properties of SMA and sandwich panel are taken as the temperature dependent and independent, respectively. Initially, the convergence and the subsequent validation of the proposed numerical model have also been checked to show the effectiveness of the presently developed higher-order model. In the present analysis, two different types of support conditions are considered for the current numerical analysis purpose and presented in Fig. 3.

The following material properties are utilised for the buckling analysis of SMA laminated composites Kumar and Singh (2009):

Composite matrix: (graphite/epoxy)

$$E_1 = 155GPa, E_2 = 8.07GPa, E_3 = E_2, G_{12} = 4.55GPa,$$

$$G_{23} = 3.25GPa, G_{31} = 4.55GPa, \nu_{12} = \nu_{13} = 0.22,$$

$$\nu_{23} = 0.3488, \alpha_0 = 10^{-6}, \alpha_1 = -0.07 \times \alpha_0, \alpha_2 = \alpha_3 = 30 \times \alpha_0$$

SMA fibres - Nitinol:  $E$  is extracted from Kumar and Singh (2009) and Park *et al.* (2004) depending on the temperature increment and the recovery stress is obtained from Park *et al.* (2004) depending on the prestrain values of the SMA fibres ( $\varepsilon_r = 1\%, 2\%$ , and  $3\%$ ) including the temperature increment.

$$E_0 = 0.1GPa, G = 24.86GPa, \nu_{12} = 0.33, \alpha_1 = 10.26 \times 10^{-6}$$

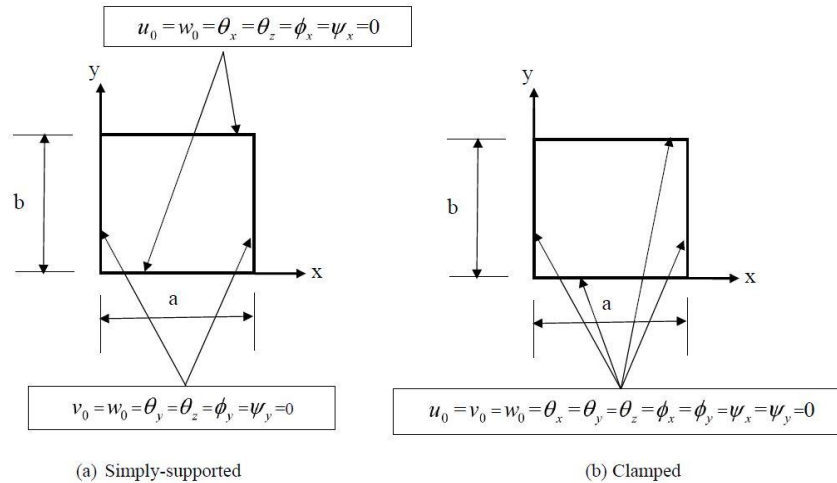


Fig. 3 End support conditions

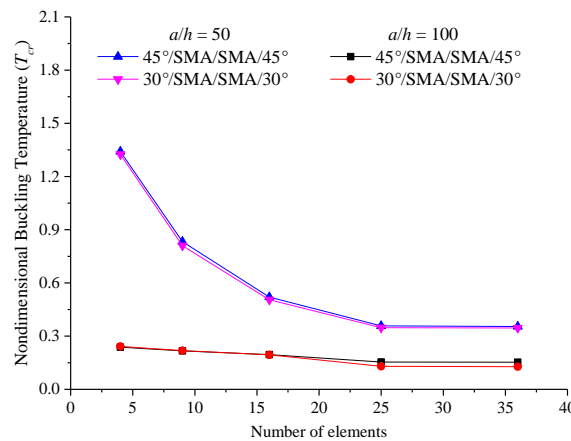


Fig. 4 Convergence of nondimensional thermal buckling temperature ( $T_{cr}$ ) of square simply supported laminated plate embedded with SMA fibre alloy

3.1 Convergence and validation study

In the present section, the convergence and the comparison behaviour of the currently developed higher-order numerical model for the SMA bonded layered sandwich structure have been obtained and discussed. Initially, the convergence responses of the present numerical results are obtained via solving a square simply-supported laminated plate structure bonded with SMA fibre. Additionally, SMA volume fractions ( $V_{SMA}$ ) and the prestrain ( $\epsilon_r$ ) values are taken as same as the reference i.e., 0.1 and 1%, respectively. Further, the nondimensional buckling temperature parameter ( $T_{cr} = 10^3 \lambda \alpha_0 \Delta T$ ) is obtained for two lamination schemes ( $45^\circ/SMA/SMA/45^\circ$  and  $30^\circ/SMA/SMA/30^\circ$ ) and two side-to-thickness ratios ( $a/h = 50$  and  $100$ ) using the material properties as same as Kumar and Singh (2009). The responses are obtained for the different numbers of elements and presented in Fig. 4. From the figure, it can be seen that the present model is showing good convergence and a  $(5 \times 5)$  mesh size is sufficient to compute the new results.

Further, to show the validity of the presently developed higher-order FEM model one example of the SMA embedded composite plate problem has been solved and presented in Table 1. The geometrical and material properties are taken as same as in the convergence analysis. It is observed from the responses that the results are in good agreement with the available published literature and the differences are within acceptable range ( $\leq 10\%$ ).

Additionally, the difference between the results may due to the kinematic models i.e., the LWT is adopted in the reference whereas the single-layer HSDT kinematic model in the present investigation.

3.2 Numerical examples:

The buckling responses are generally obtained for the square sandwich curved (cylindrical, spherical, hyperbolic, and elliptical)/flat shell panel embedded with SMA fibre using two different stacking sequences i.e.,  $SMA/0^\circ/90^\circ/Core/90^\circ/0^\circ/SMA$  and  $0^\circ/90^\circ/SMA/Core/SMA/90^\circ/0^\circ$  throughout the analysis, if

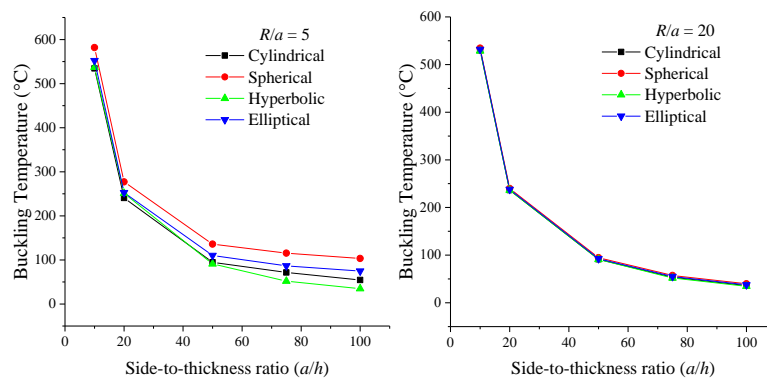


Fig. 5 Effect of side-to-thickness ratios on buckling temperature of square simply-supported (SMA/0°/90°/Core/90°/0°/SMA) sandwich shell panel embedded with SMA alloy ( $R/a = 5$  and  $20$ ,  $t_c/t_f = 20$ , and  $V_{SMA} = 0.1$ )

Table 1 Comparison study of non-dimensional thermal buckling temperature ( $T_{cr}$ ) of square simply supported laminated plate embedded with SMA fibre alloy

| Lamination Scheme | Side-to-thickness ratio ( $a/h$ ) | Present | LWT [Kumar and Singh (2009)] |
|-------------------|-----------------------------------|---------|------------------------------|
| (30°/SMA/SMA/30°) | 50                                | 0.3478  | 0.387                        |
|                   | 100                               | 0.1298  | 0.137                        |
| (45°/SMA/SMA/45°) | 50                                | 0.3577  | 0.396                        |
|                   | 100                               | 0.1541  | 0.169                        |

not stated otherwise. In addition, the structural components are assumed to be under the influence of two general support conditions (simply supported and clamped) including the same material properties as discussed in the earlier example.

The responses of curved/flat shell structures are obtained for various parameters say, the side-to-thickness ratios ( $a/h$ ), the core-to-face thickness ratios ( $t_c/t_f$ ), the curvature ratios ( $R/a$ ) and the support conditions including three different volume fractions of the SMA fibre ( $V_{SMA} = 0.1, 0.2$  and  $0.3$ ). It is worthy to mention that SMA properties for the present analysis are similar to the properties mentioned in Kumar and Singh (2009) whereas the sandwich material properties for the current analysis as same as Dehkordia and Khalili (2015). The detailed properties of the face sheet and core layer of the sandwich construction are given in the following lines.

$$\text{Face: } E_1 = 275GPa, E_2 = E_3 = 6.9GPa,$$

$$G_{12} = G_{23} = G_{13} = 6.9GPa, \nu_{12} = \nu_{13} = 0.25, \nu_{23} = 0.3$$

$$\text{Core: } E_1 = E_2 = E_3 = 0.5776GPa, G_{12} = G_{13} = 0.1079GPa,$$

$$G_{23} = 0.22215GPa, \nu_{12} = \nu_{23} = \nu_{13} = 0.0025$$

In addition, SMA recovery stress ( $\{\sigma_{sr}\}$ ) values are utilised throughout the computations according to the volume fractions of SMA i.e.,  $\epsilon_r = 1\%$ ,  $2\%$  and  $3\%$  for  $V_s = 0.1, 0.2$  and  $0.3$ , respectively.

### 3.2.1 Effect of side-to-thickness ratios

In this numerical example, the buckling temperature of the square simply-supported (SMA/0°/90°/Core/90°/0°/SMA) SMA embedded sandwich curved shell panels are obtained for five side-to-thickness ratios ( $a/h = 10, 20, 50, 75$ , and  $100$ ) and presented in Fig. 5.

In addition, the associated parameters (geometrical and material) such as two curvature ratios ( $R/a = 5$  and  $20$ ), the volume fraction of SMA ( $0.1$ ) and the core-to-face thickness ratio ( $t_c/t_f = 20$ ) included for the necessary computational purpose. The buckling temperature values are following a decreasing trend for both the parameters i.e., the side-to-thickness ratios ( $a/h$ ) and the curvature ratios ( $R/a$ ). This is because of the fact that the structural stiffness altered largely with the change in the side-to-thickness ratios as well as the curvature ratios. It is important to mention that the structural stiffness values closely associated with the geometrical and the material parameters, which, in turn, affect the final solutions. Additionally, the buckling temperature for the different geometries follows a decreasing trend i.e., spherical, elliptical, cylindrical and hyperbolic. The critical temperature characteristics can be easily visualized for  $R/a = 5$  instead of  $20$ .

### 3.2.2 Effect of curvature ratios

Now, the effect of curvature ratios on the thermal buckling responses of the simply-supported square (0°/90°/SMA/Core/SMA/90°/0°) sandwich curved shell

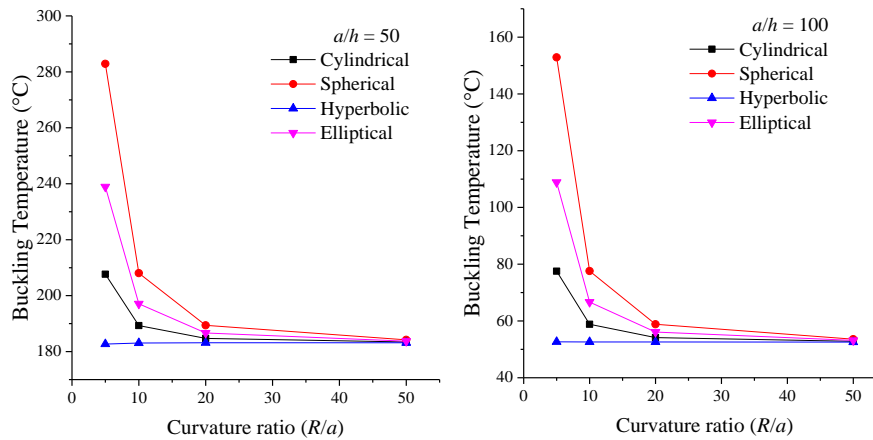


Fig. 6 Effect of curvature ratios on buckling temperature of square simply-supported ( $0/90^\circ/\text{SMA}/\text{Core}/\text{SMA}/90^\circ/0^\circ$ ) sandwich shell panel embedded with SMA alloy ( $t_c/t_f = 5$ ,  $V_{\text{SMA}} = 0.2$ )

panels embedded with SMA fibre are evaluated in this illustration and presented in Fig. 6. For the computational purpose, the necessary geometrical and material parameters are taken as: four curvature ratios ( $R/a = 5, 10, 20$  and  $50$ ), two side-to-thickness ratios ( $a/h = 50$  and  $100$ ) and  $t_c/t_f = 5$  including 0.2 part of SMA volume fraction ( $V_{\text{SMA}}$ ). The responses follow similar kind of behaviour as discussed in the earlier example i.e., the buckling temperature values follow a decreasing trend when curvature ratio increase. It is because of the fact that the structure becomes flat when the curvature ratio increase and the flat structure possesses low bending energy in comparison to the curved panel.

### 3.2.3 Effect of core-to-face thickness ratios

In this example, the buckling responses of the clamped SMA embedded sandwich curved shell panel ( $\text{SMA}/0^\circ/90^\circ/\text{Core}/90^\circ/0^\circ/\text{SMA}$ ) are computed using the current higher-order FE model and presented in Fig. 7. In order to examine the effect of the core-to-face thickness ratios on the buckling temperature, three different possible combinations of the core-to-face thickness ratios ( $t_c/t_f = 2, 10$  and  $20$ ) are employed. Additionally, the required parameter for the numerical analysis i.e., the side-to-thickness ratio ( $a/h = 50$ ), the curvature ratio ( $R/a = 5$ ) and 0.3 part of SMA fraction ( $V_{\text{SMA}}$ ) are included. The responses indicate that the buckling temperature values are increasing when the core-to-face thickness ratios ( $t_c/t_f$ ) increase irrespective of geometries and the associated parameters. In addition, the change in geometrical configurations (numbers of curvature and directions of curvature) have substantial effect on the thermal buckling strength i.e., the values follow an increasing trend progressively from the cylindrical (one curvature), the elliptical (one curvature is double of another), the hyperbolic (unequal curvature) and the spherical (equal curvature).

### 3.2.4 Effect of volume fractions of SMA

In this example, the buckling responses are computed for the clamped ( $\text{SMA}/0^\circ/90^\circ/\text{Core}/90^\circ/0^\circ/\text{SMA}$ ) sandwich curved shell panels embedded with SMA fibre and provided in Table 2. The numerical results are computed for three volume fractions of SMA ( $V_s = 0.1, 0.2$  and  $0.3$ ), one core-to-face thickness ratio ( $t_c/t_f = 20$ ), two side-to-thickness ratios ( $a/h = 10$  and  $50$ ) and two curvature ratios ( $R/a = 5$  and  $10$ ). It is understood from the results provided in Table 2, that the buckling temperature values are decreasing when both the side-to-thickness ratios ( $a/h$ ) and the curvature ratios ( $R/a$ ) increase. In addition, the buckling responses are increasing when the volume fractions of SMA fibre increase and it is obvious. Similarly, the responses declining progressively as the geometrical shape changes from spherical, hyperbolic, elliptical and cylindrical, respectively.

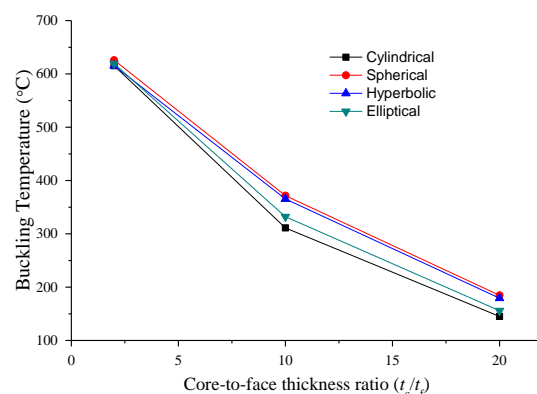


Fig. 7 Effect of core-to-face thickness ratios on buckling temperature of square clamped ( $\text{SMA}/0^\circ/90^\circ/\text{Core}/90^\circ/0^\circ/\text{SMA}$ ) sandwich shell panel embedded with SMA alloy ( $R/a=5$ ,  $a/h=50$ ,  $V_{\text{SMA}}=0.3$ )

Table 2 Effect of SMA volume fraction on buckling temperature of square clamped (SMA/0°/90°/Core/90°/0°/SMA) sandwich shell panel embedded with SMA alloy ( $t_c/t_f = 20$ )

| $V_{SMA}$ | $R/a$ | $a/h$ | Cylindrical               | Spherical | Hyperbolic | Elliptical |
|-----------|-------|-------|---------------------------|-----------|------------|------------|
|           |       |       | Buckling temperature (°C) |           |            |            |
| 0.1       | 5     | 10    | 797.4065                  | 859.101   | 853.8578   | 819.9615   |
|           |       | 50    | 145.0181                  | 184.7092  | 179.2908   | 155.7473   |
|           | 10    | 10    | 792.079                   | 813.9049  | 811.1411   | 797.9311   |
|           |       | 50    | 139.5005                  | 149.6393  | 147.7605   | 142.2788   |
| 0.2       | 5     | 10    | 797.4074                  | 859.1027  | 853.8599   | 819.9624   |
|           |       | 50    | 145.0195                  | 184.7108  | 179.2924   | 155.7488   |
|           | 10    | 10    | 792.0794                  | 813.9053  | 811.1416   | 797.9315   |
|           |       | 50    | 139.5009                  | 149.6397  | 147.761    | 142.2792   |
| 0.3       | 5     | 10    | 797.4088                  | 859.1054  | 853.8632   | 819.9638   |
|           |       | 50    | 145.0218                  | 184.7132  | 179.2948   | 155.7511   |
|           | 10    | 10    | 792.0801                  | 813.9059  | 811.1424   | 797.9321   |
|           |       | 50    | 139.5015                  | 149.6404  | 147.7616   | 142.2799   |

Table 3 Effect of support conditions on buckling temperature of square (SMA/0°/90°/Core/90°/0°/SMA) sandwich shell panel embedded with SMA alloy ( $t_c/t_f = 10$ ,  $R/a = 20$ ,  $V_{SMA} = 0.1$ )

| Support condition | $a/h$ | Buckling temperature (°C) |           |            |            |
|-------------------|-------|---------------------------|-----------|------------|------------|
|                   |       | Cylindrical               | Spherical | Hyperbolic | Elliptical |
| Simply-supported  | 10    | 605.2696                  | 609.8363  | 604.2014   | 607.1159   |
|                   | 100   | 47.4421                   | 51.5466   | 45.9164    | 49.1718    |
| Clamped           | 10    | 799.3242                  | 804.8069  | 803.7665   | 800.8255   |
|                   | 100   | 149.7639                  | 160.2246  | 158.9747   | 152.5535   |

### 3.2.5 Effect of support conditions

Table 3 represents the effect of support conditions and geometrical configuration on the buckling responses of SMA fibre embedded (SMA/0°/90°/Core/90°/0°/SMA) sandwich curved shell panels. The responses are obtained for two different support conditions i.e., all edges simply-supported and clamped. Further, few other geometrical parameters are also employed in this current example such as: the core-to-face thickness ratios ( $t_c/t_f = 10$ ), the side-to-thickness ratios ( $a/h = 10$  and  $100$ ), and the curvature ratios ( $R/a = 20$ ) including 0.1 part of SMA volume fractions ( $V_{SMA}$ ). It is observed from the responses that the buckling temperature values are higher for the clamped type support when compared to the simply supported case irrespective of the geometries and other parameters.

## 4. Conclusions

The current article investigated the buckling temperature of SMA embedded sandwich shell panel of various geometrical configurations (cylindrical, spherical, elliptical, and hyperbolic) under the influence of elevated thermal field. The buckling temperature of sandwich structural panel and the subsequent effect SMA embedding are

obtained numerically with help of a new higher-order FE model. In addition, the geometrical distortion of the panel due to the excess thermal loading is included via Green-Lagrange nonlinear strain kinematics and the model is associated with all of the higher-order terms for the sake of generality. Subsequently, the required responses are obtained computationally with the help of a home-made computer code (MATLAB) with the help of higher-order FE model. The responses are obtained by minimising the TPE and the material nonlinearity achieved through the marching technique for the temperature increment. Finally, few sets of numerical examples have been solved for various geometrical parameters utilising the layered sandwich and SMA properties to establish the improvement in structural strength and geometrical configuration.

Based on the computed numerical examples it is observed that the structural strength not only depends on SMA fraction but also affected due to other geometrical parameters and geometrical configuration. In addition, the buckling temperature of the spherical sandwich panel is higher as compared to all other geometries with or without SMA fibre.

## References

- Asadi, H., Kiani, Y., Aghdam M.M. and Shakeri, M. (2015), "Enhanced thermal buckling of laminated composite cylindrical shells with shape memory alloy", *J. Compos. Mater.*, **50**(2), 243-256.
- Babu, C.S. and Kant, T. (2000), "Refined higher order finite element models for thermal buckling of laminated composite and sandwich plates", *J. Therm. Stresses*, **23**(2), 111-130.
- Birman, V. (1997a), "Stability of functionally graded shape memory alloy sandwich panels", *Smart Mater. Struct.*, **6**, 278-286.
- Birman, V. (1997b), "Theory and comparison of the effect of composite and shape memory alloy stiffeners on stability of composite shells and plates", *Int. J. Mech. Sci.*, **39**(10), 1139-1149.
- Bouderba, B., Houari, M.S.A., Tounsi, A. and Mahmoud, S.R. (2016), "Thermal stability of functionally graded sandwich plates using a simple shear deformation theory", *Struct. Eng. Mech.*, **58**(3), 397-422.
- Bourada, M., Tounsi, A., Houari, M.S.A. and Bedia, E.A.A. (2011), "A new four-variable refined plate theory for thermal buckling analysis of functionally graded sandwich plates", *J. Sandwi. Struct. Mater.*, **14**(1), 5-33.
- Chalak, H.D., Chakrabarti, A. Sheikh, A.H. and Iqbal, M.A. (2015), "Stability analysis of laminated soft core sandwich plate using HOZT", *Mech. Adv. Mater. Struct.*, **22**(11), 897-907.
- Chikh, A., Tounsi, A., Hebali H. and Mahmoud, S.R. (2017), "Thermal buckling analysis of cross-ply laminated plates using a simplified HSDT", *Smart Mater. Syst.*, **19**(3), 289-297.
- Cook, R.D., Malkus, D.S., Plesha, M.E. and Witt, R.J. (2000), *Concepts and Applications of Finite Element Analysis*, John Wiley & Sons Pte. Ltd., Singapore.
- Dehkordia, M.B. and Khalili, S.M.R. (2015), "Frequency analysis of sandwich plate with active SMA hybrid composite face-sheets and temperature dependent flexible core", *Compos. Struct.*, **123**, 408-419.
- Fantuzzi, N., Tornabene, F., Baccocchi, M., Neves, A.M.A. and Ferreira, A.J.M. (2017), "Stability and accuracy of three Fourier expansion-based strong form finite elements for the free vibration analysis of laminated composite plates", *Int. J. Numer. Meth. Engng*, DOI: 10.1002/nme.5468.
- Fazzolari, F.A. and Carrera, E. (2013), "Thermo-mechanical buckling analysis of anisotropic multilayered composite and sandwich plates by using refined variable-kinematics theories", *J. Therm. Stresses*, **36**(4), 321-350.
- Hassanli, S. and Samali, B. (2016), "Buckling analysis of laminated composite curved panels reinforced with linear and non-linear distribution of shape memory alloys", *Thin Wall. Struct.*, **106**, 9-17.
- Juhasz, Z. and Szekrenyes, A. (2015a), "Progressive buckling of a simply supported delaminated orthotropic rectangular composite plate", *Int. J. Solids Struct.*, **69-70**, 217-229.
- Juhasz, Z. and Szekrenyes, A. (2015b), "Estimation of local delamination buckling in orthotropic composite plates using Kirchhoff plate finite elements", *Math. Probl. Eng.*, DOI: 10.1155/2015/749607.
- Kaci, A., Draiche, K., Zidi, M., Houari, M.S.A. and Tounsi, A. (2013), "An efficient and simple refined theory for nonlinear bending analysis of functionally graded sandwich plates", *J. Appl. Mech. Tech. Phys.*, **54**(5), 847-856.
- Kant, T. and Babu, C.S. (2000) "Thermal buckling analysis of skew fibre-reinforced composite and sandwich plates using shear deformable finite element models", *Compos. Struct.*, **49**, 77-85.
- Katariya, P.V. and Panda, S.K. (2016) "Thermal buckling and vibration analysis of laminated composite curved shell panel", *Aircr Eng Aerosp Tec.*, **88**(1), 97-107.
- Kettaf, F.Z., Houari, M.S.A., Benguediab M. and Tounsi, A. (2013), "Thermal buckling of functionally graded sandwich plates using a new hyperbolic shear displacement model", *Steel Compos. Struct.*, **15**(4), 399-423.
- Kumar, S.K. and Singh, B.N. (2009), "Thermal buckling analysis of SMA fibre-reinforced composite plates using layerwise model", *J. Aerosp. Eng.*, **22**, 342-353.
- Kuo, S.Y., Shiau, L.C. and Chen K.H. (2009), "Buckling analysis of shape memory alloy reinforced composite laminates", *Compos. Struct.*, **90**, 188-195.
- Lee, H.J. and Lee, J.J. (2000), "A numerical analysis of the buckling and postbuckling behavior of laminated composite shells with embedded shape memory alloy wire actuators", *Smart Mater. Struct.*, **9**, 780-787.
- Meiche, N.E., Tounsi, A., Ziane, N., Mechab, I. and Bedia, E.A.A. (2011), "A new hyperbolic shear deformation theory for buckling and vibration of functionally graded sandwich plate", *Int. J. Mech. Sci.*, **53**, 237-247.
- Panda, S.K. (2009), "Nonlinear Vibration Analysis of Thermally Post-buckled Composite Shell Panels with and without Shape Memory Alloy Fibres", *Doctoral Dissertation. Indian Institute of Technology Kharagpur, West Bengal, India.*
- Panda, S.K. and Singh, B.N. (2013), "Nonlinear finite element analysis of thermal post-buckling vibration of laminated composite shell panel embedded with SMA fibre", *Aerosp. Sci. Technol.*, **29**, 47-57.
- Parhi, A. and Singh, B.N. (2016), "Nonlinear free vibration analysis of shape memory alloy embedded laminated composite shell panel", *Mech. Adv. Mater. Struct.*, DOI: 10.1080/15376494.2016.1196777.
- Park, J.S., Kim, J.H. and Moon, S.H. (2004), "Vibration of thermally post-buckled composite plates embedded with shape memory alloy fibers", *Compos. Struct.*, **63**(2), 179-188.
- Reddy, J.N. (2004), *Mechanics of Laminated Composite: Plates and Shells - Theory and Analysis*, CRC Press, Boca Raton FL.
- Sciuva, M.D. and Carrera, E. (1990), "Static buckling of moderately thick anisotropic laminated and sandwich cylindrical shell panels", *AIAA J.*, **28**(10), 1782-1793.
- Shao, C. Cao, D. Xu, Y. and Zhao, H. (2016), "Flutter and thermal buckling analysis for composite laminated panel embedded with shape memory alloy wires in supersonic flow", *Int. J. Aerosp. Eng.*, DOI: 10.1155/2016/8562716.
- Singh, V. K. and Panda, S.K. (2015), "Large amplitude vibration behaviour of laminated composite spherical shell embedded with piezoelectric layer", *Smart Mater. Syst.*, **16**(5), 853-872.
- Thai, C.H., Ferreira, A.J.M., Carrera, E. and Nguyen-Xuan, H. (2013), "Isogeometric analysis of laminated composite and sandwich plates using a layerwise deformation theory", *Compos. Struct.*, **104**, 196-214.
- Topal, U. (2009b), "Multiobjective optimization of laminated composite cylindrical shells for maximum frequency and buckling load", *Mater. Design*, **30**, 2584-2594.
- Topal, U. (2012), "Thermal buckling load optimization of laminated plates with different intermediate line supports", *Steel Compos. Struct.*, **13**(3), 207-223.
- Topal, U. and Uzman, U. (2009a), "Thermal buckling load optimization of angle-ply laminated cylindrical shells", *Mater. Design*, **30**, 532-536.
- Tornabene, F., Fantuzzi, N. and Baccocchi, M. (2014), "The strong formulation finite element method: stability and accuracy", *Fract. Struct. Integ.*, **29**, 251-265.
- Tornabene, F., Fantuzzi, N., Viola, E. and Batra, R.C. (2015), "Stress and strain recovery for functionally graded free-form and doubly-curved sandwich shells using higher-order equivalent single layer theory", *Compos. Struct.*, **119**, 67-89.
- Zhang, Y. and Zhao, Y.P. (2007a), "A discussion on modeling

shape memory alloy embedded in a composite laminate as axial force and elastic foundation”, *Mater. Design*, **28**, 1016-1020.

Zhang, Y. and Zhao, Y.P. (2007b), “A study of composite beam with shape memory alloy arbitrarily embedded under thermal and mechanical loadings”, *Mater. Design*, **28**, 1096-1115.

CC